THE JOURNAL OF BIOLOGICAL CHEMISTRY VOL. 285, NO. 24, pp. 18301–18308, June 11, 2010

Neuroprotectin D1 Induces Dephosphorylation of Bcl-x_L in a PP2A-dependent Manner during Oxidative Stress and Promotes Retinal Pigment Epithelial Cell Survival*

Received for publication, December 15, 2009, and in revised form, April 1, 2010 Published, JBC Papers in Press, April 2, 2010, DOI 10.1074/jbc.M109.095232

Rajee Antony, Walter J. Lukiw, and Nicolas G. Bazan[1]

From the Neuroscience Center of Excellence, Louisiana State University Health Sciences Center, New Orleans, Louisiana 70112

Retinal pigment epithelial (RPE) cell integrity is critical for the survival of photoreceptor cells. Bcl-x_L is a major anti-apoptotic Bcl-2 protein required for RPE cell survival, and phosphorylation of Bcl-x_L at residue Ser-62 renders this protein pro-apoptotic. In this study, we identify serine/threonine protein phosphatase 2A (PP2A) as a key regulator of Bcl-x_L phosphorylation at residue Ser-62 in ARPE-19 cells, a spontaneously arising RPE cell line in which Bcl-x_L is highly expressed. We found that either PP2A inhibitor okadaic acid or depletion of catalytic subunit α of PP2A (PP2A/Cα) by small interfering RNA enhanced Bcl-x_L phosphorylation when activated with hydrogen peroxide and tumor necrosis factor α-induced oxidative stress. Disruption of PP2A/Cα exacerbated oxidative stress-induced apoptosis. PP2A/Cα colocalized and interacted with S62Bcl-x_L in cells stressed with H_2O_2/tumor necrosis factor α. By contrast, the omega-3 fatty acid docosahexaenoic acid derivative, neuroprotectin D1 (NPD1), a potent activator of survival signaling, down-regulated oxidative stress-induced phosphorylation of Bcl-x_L by increasing protein phosphatase activity. NPD1 also attenuated the oxidative stress-induced apoptosis by knockdown of PP2A/Cα and increased the association of PP2A/Cα with S62Bcl-x_L as well as total Bcl-x_L. NPD1 also enhanced the heterodimerization of Bcl-x_L with its counterpart, pro-apoptotic protein Bax. Thus, NPD1 modulates the activation of this Bcl-2 family protein by dephosphorylating in a PP2A-dependent manner, suggesting a coordinated, NPD1-mediated regulation of cell survival in response to oxidative stress.

Retinal pigment epithelial (RPE)[2] cell integrity is necessary for the survival of rod and cone photoreceptors, and these cells accomplish a myriad of functions, including transport of retinol and of the essential omega-3 fatty acid, docosahexaenoic acid, and also transport of nutrients between photoreceptors and the choriocapillaries (1, 2). Our laboratory has shown that RPE cells, when induced with oxidative stress, produce and release to the media a stereospecific oxygenation product of docosahexaenoic acid, named neuroprotectin D1 (NPD1) (3–6). Hence, NPD1 is a pleiotropic modulator of inflammation resolution (7). NPD1 up-regulates anti-apoptotic proteins (Bcl-2, Bcl-x_L) and down-regulates pro-apoptotic proteins (Bax, Bad) in ARPE-19 cells upon exposure to hydrogen peroxide/tumor necrosis factor α (H_2O_2/TNFα)-induced oxidative stress (3, 4). Under these conditions, NPD1 inhibits cytokine-mediated pro-inflammatory gene induction (3, 8) and oxidative stress-induced apoptosis and also promotes RPE cell survival (9, 10). Oxidative stress (leading to apoptosis), neovascularization, and lipid peroxidation are involved in neurodegenerative diseases, including age related-macular degeneration (11–14).

Apoptotic pathway activation comprises well orchestrated interactions between the Bcl-2 anti-apoptotic (Bcl-2 and Bcl-x_L) and pro-apoptotic (Bax and Bad) proteins. Bcl-2 and Bcl-x_L protect cells from apoptosis, whereas Bax and Bad promote apoptosis (15, 16). Bcl-x_L regulates apoptosis by undergoing post-translational modifications, which include phosphorylation and heterodimerization with pro-apoptotic proteins (Bax and Bad), and by subcellularly localizing in the mitochondria (17–19). Bcl-x_L is phosphorylated at residue (Ser-62) through c-Jun N-terminal protein kinase (JNK) in cancer cell lines in response to anti-mitotic drugs (17, 20–22), and in turn, its anti-apoptotic function is abolished. Moreover, Bcl-x_L phosphorylation is a universal response to microtubule damage. However, the involvement of a physiological protein phosphatase in the dephosphorylation of Bcl-x_L, as well as mediators that modulate Ser-62 removal, remains unclear.

Protein phosphatase 2A (PP2A), a serine/threonine protein phosphatase, has been implicated in the dephosphorylation of Bcl-2 family proteins (23–25). PP2A is a heterotrimer composed of a catalytic (C-subunit), a structural (A-subunit), and a regulatory (B-subunit) subunit. The A- and B-subunits are ubiquitously expressed and evolutionarily conserved. The B-subunit defines the specific PP2A substrate target and its cellular localization (26). The B-subunit targets the catalytic complex (A- and C-subunits) to intracellular sites such as microtubules, the nucleus, and the cytoplasm (27, 28). PP2A has been shown to be the major phosphatase involved in the dephosphorylation of Bad (25), leading to apoptosis. Moreover, the catalytic subunit of PP2A alone is sufficient to dephosphorylate Bcl-2 (29) and Bax, triggering cell death (30).

Although the involvement of PP2A in the regulation of Bcl-x_L protein expression is known (31, 32), knowledge of protein phosphatases that dephosphorylates Bcl-x_L is scarce, par-

* This work was supported, in whole or in part, by National Institutes of Health Grant R01 EY005121 through the NEI, United States Public Health Service.

[1] To whom correspondence should be addressed: Neuroscience Center of Excellence, Louisiana State University Health Sciences Center, 2020 Gravier St., Ste. D, New Orleans, LA 70112. Tel.: 504-599-0831; E-mail: nbazan@lsuhsc.edu.

[2] The abbreviations used are: RPE, retinal pigment epithelial; Bcl-2, B-cell lymphoma protein-2; Bcl-x_L, Bcl-2-like 1; BH, Bcl-2 homology domain; JNK, c-Jun N-terminal protein kinase; PP2A, protein phosphatase 2A; PP2A/Cα, protein phosphatase 2A, catalytic subunit α; NPD1, neuroprotectin D1; siRNA, small interfering RNA; TNFα, tumor necrosis factor α; PBS, phosphate-buffered saline.

ticularly in response to apoptotic stimuli (33, 34). Thus, given the potent bioactivity of NPD1 on the Bcl-2 family proteins (3, 4) during oxidative stress, it seems that NPD1 is key in ARPE-19 cell survival. The present study was undertaken to examine the effect of NPD1 in modulating the phosphorylation of Bcl-x_L and to identify the specific species of protein phosphatase involved during induced oxidative stress in ARPE-19 cells.

EXPERIMENTAL PROCEDURES

Cell Culture—ARPE-19 cells (ATCC-CRL-2302) were cultured and maintained at 37 °C in Dulbecco's modified Eagle's medium/F12 supplemented with 10% fetal bovine serum in a humidified atmosphere containing 5% CO_2. NPD1 was a kind gift from Dr. Nicos Petasis, Loker Hydrocarbon Research Institute, University of Southern California, Los Angeles, CA.

Subcellular Fractionation—ARPE-19 cells were grown in six-well plates to 100% confluence, serum-starved for 18 h, and stimulated with 200 μM H_2O_2, 10 ng/ml TNFα according to the experimental design. Cells were then washed once with ice-cold PBS and collected by scraping into 100–300 μl of cytosolic lysis buffer (20 mM Tris, pH 7.5; 150 mM NaCl; 10 mM EDTA; 200 μM Na_3VO_4; 10 mM NaF; 5 μg/ml leupeptin; 1 mM phenylmethylsulfonyl fluoride; and 10% glycerol). Cells were further lysed with 20 strokes of a Dounce homogenizer, and supernatants were collected as cytosolic fraction after centrifugation for 30 min at 50,000 rpm at 4 °C. Pellets were then washed once with ice-cold PBS and homogenized in membrane lysis buffer (cytosolic lysis buffer containing 1% Nonidet P-40) using 20 strokes of a Dounce homogenizer. After incubation on ice for 20 min with interval shaking and centrifugation for 30 min at 50,000 rpm and 4 °C, the supernatants were collected as the membrane fraction. The whole cell lysates were prepared by scraping the cells into 100–300 μl of membrane lysis buffer, incubated on ice for 20 min with shaking every 5 min, and centrifuged for 30 min at 14,000 rpm and 4 °C.

Western Blot Analysis—The protein content was estimated with protein assay reagent (Bio-Rad) according to the manufacturer's instructions. Equal amounts of cell extract protein from different conditions (10–20 μg) were loaded onto and separated by 8–16% SDS-PAGE ready-made gels. On fractionation, proteins were transferred to polyvinylidene difluoride membranes in a Trans-Blot apparatus. Membranes were blocked with 5% skim milk in PBS containing 0.1% Tween 20 for 1 h at room temperature or overnight at 4 °C. Membranes were then incubated with monoclonal or polyclonal antibody raised against the protein of interest for 1 h at room temperature or overnight at 4 °C followed by three washes with PBS containing 0.1% Tween 20. The immunoreactivity of the primary antibodies Bcl-x_L (Cell Signaling, Danvers, MA), S62Bcl-x_L (Upstate Biotech Millipore, Billerica, MA), Bax (Cell Signaling), PP2A/C (BD Biosciences), voltage density anion channels (Calbiochem), and I1PP2A and I2PP2A antibodies sc-5652 (C-18) and sc-5655 (E15), respectively, (Santa Cruz Biotechnology, Santa Cruz, CA) and actin (Sigma) was visualized with a secondary anti-rabbit (BD Transduction Laboratories) or anti-mouse (Santa Cruz Biotechnology) antibodies conjugated with horseradish peroxidase and subsequent development with ECL Plus (Amersham Biosciences) and autoradiography on X-OMART AR films. The bands were scanned and quantified by the Gel Doc system using the Quantity One software, or intensity analysis was carried out using Fujifilm MultiGauge Version 3.0.

Immunoprecipitation—For immunoprecipitation with Bcl-x_L and S62Bcl-x_L antibody (Thermo Scientific), protein A-Sepharose slurry (Thermo Scientific) was washed with 1× PBS and incubated with Bcl-x_L and S62Bcl-x_L antibody or normal rabbit IgG (control) for 1 h at 4 °C. After three washes with lysis buffer, the beads were incubated with whole cell lysates (0.5 mg of total protein) for 1 h and then washed three times with lysis buffer. The proteins were then eluted by boiling in 1× SDS-sample buffer.

Total PP1/PP2A Phosphatase Activity Assay—Total PP1/PP2A activity was measured using a Malachite Green PP1/PP2A phosphatase assay kit (Upstate Biotech Millipore), which is optimized for PP1 and PP2A but cannot distinguish between these two enzymes. The assay is based on dephosphorylation of a phosphopeptide substrate (K-R-pT-I-R-R); the released phosphate binds to malachite green, leading to increased absorbance at 650 nm. Cultured ARPE-19 cells were treated accordingly and scraped into phosphatase extraction buffer (20 mM imidazole-HCl, 2 mM EDTA, and 2 mM EGTA, pH 7.0, with 10 mg/ml aprotinin, leupeptin, 1 mM benzamidine, and 1 mM phenylmethylsulfonyl fluoride) and then sonicated for 10 s and centrifuged at 2000 × *g* for 5 min. Resulting cell lysates were used for the phosphatase activity assay. Absorbance values at 650 nm were subtracted by that of negative control (no cell lysate added).

siRNA Transfection—Knockdown of PP2A/C siRNA was performed by reverse transfection of PP2A/Cα (Ambion, Austin, TX) into retinal pigment epithelial cells by using siPORT NeoFX transfection reagent according to the manufacturer's instruction. A control siRNA (nonhomologous to any known gene sequence) was used as a negative control. The transfected cells were incubated at 37 °C for 48 h and then serum-starved for 18 h and subsequently treated with H_2O_2/TNFα. Bcl-x_L phosphorylation was assessed by Western blotting.

Hoechst Staining and Apoptosis Analysis—Control siRNA- and PP2A/C-transfected ARPE-19 cells were treated accordingly, washed with PBS, and fixed for 10 min with methanol. Cells were incubated with 2 μg/ml Hoechst 33258 for 15 min at room temperature. Single plane images were taken using a DIAPHOT 200 microscope (Nikon, Melville, NY) with fluorescence optics. Images were recorded using a Hamamatsu color chilled 3CCD camera (Bridgewater, NJ) and PhotoShop software, Version 5.0 (Adobe Systems, Mountain View, CA) (5, 10).

RESULTS

Phosphorylation of Bcl-x_L Protein at Residue Ser-62—ARPE-19 cells were treated with 200 μM H_2O_2/TNFα for 5 min to 90 min, and whole cell extracts were prepared and subjected to immunoblotting with phospho-specific Ser-62 antibody to Bcl-x_L. The phosphorylated form of Bcl-x_L was observed as early as 15 min with a significant up-regulation after 30 min of oxidative stress (Fig. 1*A*). The total Bcl-x_L protein levels after a 90-min exposure to H_2O_2/TNFα were similar to those in control cells, suggesting that the phosphorylation and dephosphorylation cycle does not promote net protein

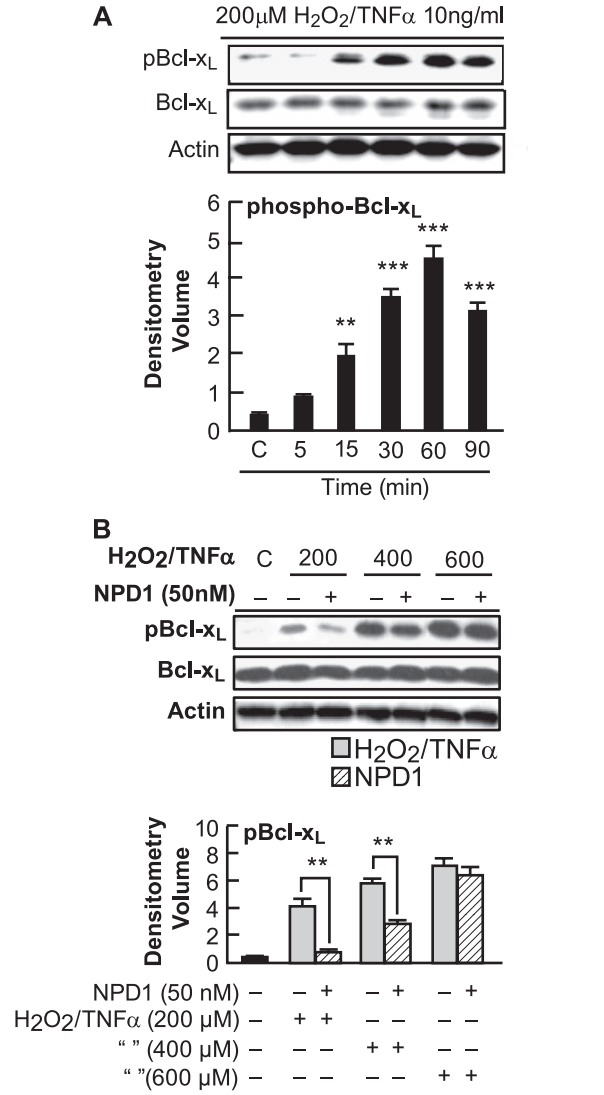

FIGURE 1. **Analysis of Bcl-x_L protein phosphorylation.** *A*, phosphorylation of Bcl-x_L protein at residue Ser-62 in ARPE-19 cells in response to oxidative stress. ARPE-19 cells were serum-starved for 18 h and treated with 200 μM H_2O_2/TNFα for 5, 15, 30, 60, and 90 min. Immunoblot represents S62Bcl-x_L, total Bcl-x_L, and actin. Phospho-Bcl-x_L was significantly up-regulated at 30 min. *Error bars* indicate ± S.E. of three sets of different experiments. ***, $p < 0.001$, **, $p < 0.01$, when compared with stress-treated cells. *C* indicates control. *B*, NPD1 down-regulated the oxidative stress-induced phosphorylation of Bcl-x_L at residue Ser-62. ARPE-19 cells were serum-starved for 18 h and then induced with 200, 400, and 600 μM H_2O_2 and 10 ng/ml TNFα in the presence and absence of NPD1 (50 nM) for 30 min. Whole cell extracts were prepared and tested by Western blot for the presence of S62Bcl-x_L and total Bcl-x_L. Also, actin was used as a loading control. Phosphorylation of Bcl-x_L was significantly down-regulated in the presence of 200 μM H_2O_2/TNFα. No statistical difference was observed in cells treated with 600 and 800 (data not shown) μM H_2O_2/TNFα. *Error bars* indicate ± S.E. of three independent experiments. **, $p < 0.01$, when compared with stress-treated cells.

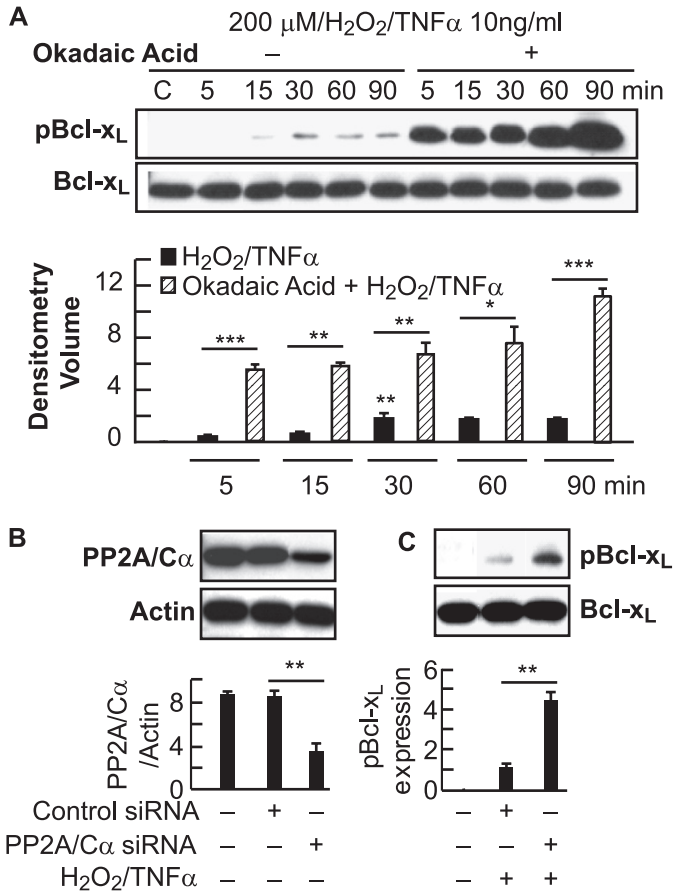

FIGURE 2. **Analysis of PP1/PP2a inhibitor effects.** *A*, PP1/PP2A inhibitor increased the oxidative stress-induced dephosphorylation of Bcl-x_L in a time-dependent manner. ARPE-19 cells were serum-starved for 18 h and then induced with 200 μM H_2O_2 and 10 ng/ml TNFα in the presence and absence of PP1/PP2A specific inhibitor okadaic acid (100 nM) at 5, 15, 30, 60, and 90 min. Whole cell lysates were prepared and tested for the presence of phospho-Bcl-x_L and total Bcl-x_L. *Upper*, representative Western blot; *lower*, summary data. *C* indicates control. *B*, PP2A/Cα phosphorylates endogenous Bcl-x_L in ARPE-19 cells. *Error bars* indicate ± S.E. of three independent experiments. ***, $p \leq 0.0001$, **, $p < 0.01$, and *, $p < 0.05$, when compared with stress- and okadaic acid-treated cells. ARPE-19 cells were transfected with scrambled siRNA or with siRNA selective for PP2A catalytic subunit α. Expression levels of endogenous PP2A/Cα were analyzed by Western blot (*upper*) and summary data (*lower*) panels. *Error bars* indicate ± S.E. of three independent experiments. **, $p < 0.005$, when compared with control siRNA-treated cells. *C*, ARPE-19 cells were incubated with or without H_2O_2/TNFα for 30 min. Proteins were separated by SDS-PAGE and analyzed by immunoblotting with Ser-62 and total Bcl-x_L antibodies (*upper*). Phosphorylation of Bcl-x_L was significantly up-regulated in the cells treated with PP2A/Cα-siRNA when compared with the scrambled sequence (*lower*). *Error bars* indicate ± S.E. of three independent experiments. **, $p < 0.005$, when compared with control siRNA-treated cells.

synthesis or degradation. To explore the involvement of NPD1 in the phosphorylation of Bcl-x_L, we stimulated cells with 200–600 μM H_2O_2/TNFα for 30 min and assessed the immunoblots for S62Bcl-x_L. The phospho-Bcl-x_L was up-regulated in an H_2O_2 dose-dependent manner, and interestingly, NPD1 down-regulated the phosphorylation of Bcl-x_L at 200 μM H_2O_2 (Fig. 1*B*).

Endogenous Inhibitors of PP2A Activity—Inhibitor 1 of PP2A (I1PP2A; 32 kDa) and inhibitor 2 of PP2A (I2PP2A; 39 kDa), endogenous noncompetitive inhibitors of PP2A (49, 50), showed no significant difference between control or stressed ARPE-19 cells when compared against β-actin levels in the same sample (data not shown).

Dephosphorylation of Bcl-x_L by PP2A in Response to Oxidative Stress—To define the involvement of PP2A in Bcl-x_L phosphorylation, we used okadaic acid, a specific inhibitor for PP2A. Treatment of ARPE-19 cells with H_2O_2/TNFα in the presence of okadaic acid increased the phosphorylation of Bcl-x_L, and the endogenous amount of Bcl-x_L was not altered (Fig. 2*A*). Because PP2A catalyzes Ser-62 dephosphorylation in response to oxidative stress, we further explored the possibility of

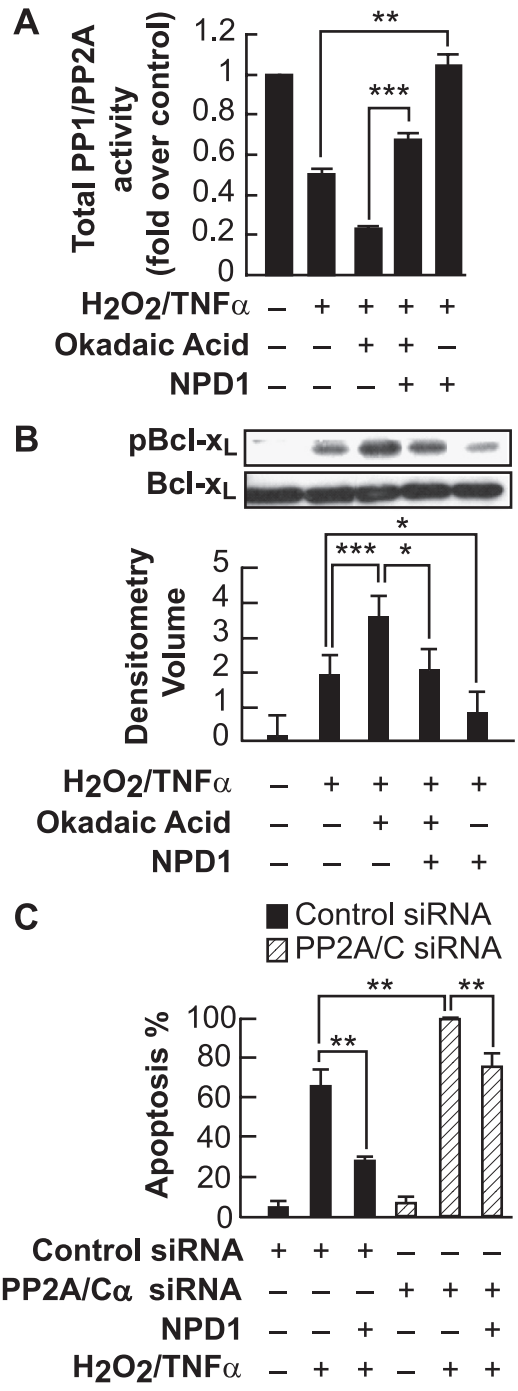

FIGURE 3. **NPD1 treatment increases PP1/PP2A phosphatase activity.** *A*, ARPE-19 cells were untreated or stimulated with H_2O_2/TNFα in the presence and absence of NPD1 for 30 min, and equal amounts of cell lysate proteins were analyzed by the Malachite Green PP1/PP2A phosphatase assay (see "Experimental Procedures"). PP1/PP2A inhibitor okadaic acid was used as a positive control. PP1/PP2A phosphatase activity was normalized to untreated control. The bar graph shows phosphate release normalized to control. *Error bars* indicate ± S.E. of three independent experiments. **, $p < 0.01$, ***, $p < 0.001$. *B*, NPD1 down-regulated the increased phosphorylation of Bcl-x_L induced by the PP1/PP2A inhibitor in response to oxidative stress. ARPE-19 cells were serum-starved for 18 h and then induced with H_2O_2/TNFα in the presence and absence of okadaic acid and NPD1 for 30 min and tested for the presence of phospho-Bcl-x_L and total Bcl-x_L. *Error bars* indicate ± S.E. of three independent experiments. ***, $p < 0.001$, *, $p < 0.05$, when compared with stress- and okadaic acid-treated samples. *C*, specific knockdown of PP2A/C expression by siRNA increased cell death. ARPE-19 cells expressing PP2A/C siRNA or control siRNA were serum-starved for 18 h and treated with 200 μM H_2O_2/TNFα in the presence and absence of NPD1 (50 nM) for 24 h. Apoptosis was assessed by counting Hoechst-positive cells. Data represent the percentage of Hoechst-positive cells to total cell count. The *bars* represent the means ± S.E. of 12 fields of four sample sets. *Error bars* indicate ± S.E. of three independent experiments. **, $p < 0.005$, when compared with H_2O_2/TNFα- and siRNA-treated samples.

involvement of a specific subunit of PP2A, the catalytic subunit α. To test this, we assayed Ser-62 dephosphorylation during oxidative stress under PP2A/Cα ablation conditions using siRNA. When compared with controls, the knockdown of endogenous PP2A/Cα protein (Fig. 2*B*) in ARPE-19 cells indeed abolishes the Ser-62 dephosphorylation in response to oxidative stress (Fig. 2*C*). These results suggest that PP2A/Cα plays a role in the dephosphorylation of Bcl-x_L at Ser-62 in response to oxidative stress.

Effect of NPD1 on PP1/PP2A Phosphatase Activity—To further define the NPD1-mediated dephosphorylation of Bcl-x_L, we assayed PP1/PP2A phosphatase activity in ARPE-19 cells. Cells were induced with oxidative stress in the presence and absence of NPD1, and phosphate-free cell lysates were prepared (35). In H_2O_2/TNFα-treated cells, the total PP1/PP2A phosphatase activity was decreased, and elevated phosphatase activity was observed in cells treated with NPD1 when compared with H_2O_2/TNFα-treated cells (**, $p < 0.01$). Moreover, when cells were treated with okadaic acid, protein phosphatase activity was decreased dramatically. On the other hand, protein phosphatase activity increased significantly (***, $p < 0.001$) when compared with cells treated with okadaic acid in the presence of NPD1 (Fig. 3*A*). The same experimental design was followed, and whole cell lysates were extracted to determine the level of Ser-62 phosphorylation of Bcl-x_L. NPD1 down-regulated the phosphorylation of Bcl-x_L when cells were induced with oxidative stress in the presence of okadaic acid, albeit to a lesser extent than in cells exposed to oxidative stress alone (Fig. 3*B*), consistent with the increased PP1/PP2A phosphatase activity. Thus, PP1/PP2A phosphatase activity is decreased when ARPE-19 cells are induced with oxidative stress, associated with enhanced phosphorylation of Ser-62 Bcl-x_L.

To test whether PP2A-mediated Bcl-x_L dephosphorylation is directly involved in ARPE-19 cell survival, cells were transfected with control siRNA and PP2A/C siRNA and treated with H_2O_2/TNFα in the presence and absence of NPD1. Specific disruption of PP2A/C exacerbated apoptosis in the presence of H_2O_2/TNFα when compared with control-treated cells. NPD1 decreased the percentage of apoptosis in control siRNA as well as PP2A/C siRNA-treated samples (Fig. 3*C*). These findings strongly suggest that PP2A may act, in part, as a Bcl-x_L phosphatase that regulates NPD1-mediated Bcl-x_L dephosphorylation in ARPE-19 cells, resulting in enhanced cellular survival.

Oxidative Stress Induces Subcellular Localization of Bcl-2 Family Proteins—To examine the impact of oxidative stress on the subcellular localization of S62Bcl-x_L and Bcl-x_L in ARPE-19 cells, cytosol- and mitochondria-enriched fractions were prepared as described under "Experimental Procedures." Voltage density anion channels (*VDAC*) were used to test the purity of cytosolic fractions and as a mitochondrial marker (Fig. 4). Moreover, in the cytosol, phosphorylation of residue Ser-62

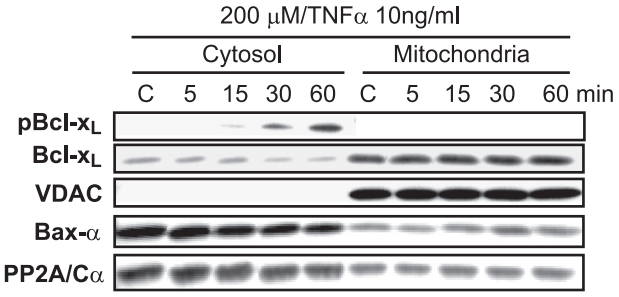

FIGURE 4. **Time-dependent oxidative stress-induced subcellular localization of S62Bcl-x_L, Bcl-x_L, and Bax-α in ARPE-19 cells.** We used biophysical centrifugation methods to ascertain cytosolic or mitochondrial compartmentalization (see "Experimental Procedures"). S62Bcl-x_L was localized in the cytosol as early as 15 min after stress and was found to be absent in mitochondrial fractions. Unphosphorylated Bcl-x_L was localized mostly in the mitochondria. Bax was predominantly present in the cytosol, and a smaller fraction was translocated to the mitochondria after 30 min of oxidative stress. Mitochondrial fractions were assessed by the mitochondrial marker, voltage density anion channels (*VDAC*). Oxidative stress also promoted translocation of PP2A/Cα to the mitochondrial membrane. *C* indicates control.

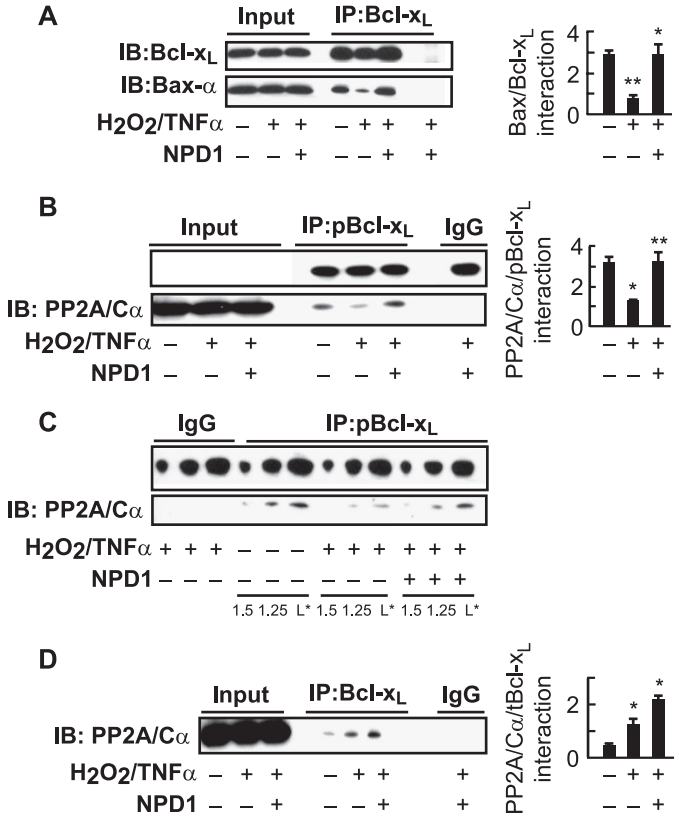

FIGURE 5. **NPD1 enhanced the heterodimerization of Bax-α with Bcl-x_L in ARPE-19 cells.** *A*, antibodies used for precipitation (*IP*) and for immunoblots (*IB*) are indicated. Immunoblots for Bax-α transcript from ARPE-19 cells were treated with 200 μM H_2O_2/TNFα in the presence and absence of NPD1 (50 nM) after immunoprecipitation. Each panel shows the initial (starting) lysate, indicating precipitate probed with Bax-α and IgG precipitate (*left panels*) with summary data on the *right*. *Error bars* indicate ± S.E. of three independent experiments. **, $p < 0.001$ and *, $p < 0.05$, when compared with control- and stress-treated cells. *B*, NPD1 increased the interaction of S62Bcl-x_L and PP2A/Cα. ARPE-19 cells were serum-starved for 18 h and induced with oxidative stress in the presence and absence of NPD1, and phospho-Bcl-x_L was used for immunoprecipitation (*left*) with summary data on the *right*. **, $p < 0.005$ and *, $p < 0.05$, when compared with control- and stress-treated cells. *C*, *L** indicates loading. *D*, NPD1 consistently increased the interaction of total Bcl-x_L with PP2A/Cα. Cells were serum-starved and induced with oxidative stress in the presence and absence of NPD1 and total Bcl-x_L was immunoprecipitated (*left*) with summary data on the *right*. *, $p < 0.05$, when compared with control- and stress-treated cells.

was detected as early as 15 min with a significant up-regulation at 60 min (Fig. 4), consistent with the up-regulation observed in whole cell lysates of oxidative stress-induced ARPE-19 cells (Fig. 1*A*). Unphosphorylated Bcl-x_L was localized predominantly to the mitochondrial fractions in H_2O_2/TNFα-treated cells, and a minimal expression of Bcl-xL was observed in the cytosol (Fig. 4). In Fig. 4, we note that over the time course studied, Bcl-x_L is decreasing in the cytosol fraction as it is modestly increasing in the mitochondrial fraction, suggestive of a transition from cytosolic to mitochondrial compartments. The possibility that S62Bcl-x_L and Bcl-x_L are also present in other subcellular organelles remains to be examined. After H_2O_2/TNFα treatment, the phosphorylated form of Bcl-x_L was found to be present in the cytosolic fraction, indicating that no significant subcellular redistribution had occurred. Thus, an antibody specific to the PP2A/Cα subunit was used to ascertain the cytosolic localization. In control cells, the maximum level of expression was observed (Fig. 4), consistent with the absence of residue Ser-62 phosphorylation of Bcl-x_L. In oxidative stress-induced cells, a down-regulation in the expression pattern of PP2A/C was observed as a function of time of up to 60 min. PP2A/C was also observed to be translocated to the mitochondria in a modest manner. Whether there are changes in PP2A/C expression at longer time points and whether other mechanisms are involved in modulating PP2A/C expression under these experimental conditions are currently not known and are the subject of ongoing research work.

NPD1 Promotes Heterodimerization of Bax with Bcl-x_L—Upon translocation to the mitochondria, Bax forms homodimers to promote cell death and heterodimers with other Bcl-2 family members, blocking apoptosis (18, 36, 37). To determine the subcellular localization of the pro-apoptotic protein Bax, ARPE-19 cells were induced with H_2O_2/TNFα, and Bax immunoreactivity was analyzed. We studied Bax using a monoclonal antibody, which detects an epitope 12–24 at the N terminus in the vicinity of the dimerization domain of Bax (38). Although Bax was predominantly localized in the cytosol of unstimulated and oxidative stress-induced cells, it was also found to be translocated to the mitochondria after 30 min of oxidative stress, consistent with a gradual decrease in the cytosolic fractions (Fig. 4). To evaluate the impact of oxidative stress on the assembly of Bax with Bcl-x_L, we performed coimmunoprecipitation with an anti-Bcl-x_L antibody and probed for Bax-α. Oxidative stress-induced ARPE-19 cells exhibited a decrease in Bax-Bcl-x_L assembly when compared with untreated cells after 30 min. Moreover, NPD1 promoted the heterodimerization of Bax and Bcl-x_L in oxidative stress-induced cells (Fig. 5*A*). These findings are consistent with the possibility that NPD1 disabled Bax from forming homodimers, thereby inhibiting the release of cytochrome *c* from the mitochondrial outer membrane to augment cell death. Hence, the availability of Bax to interact with Bcl-x_L was enhanced.

NPD1 Promotes Assembly of PP2A/C with Bcl-x_L—PP2A promotes cell survival via dephosphorylation of anti-apoptotic proteins such as Bcl-2 (39). To further investigate the correlation between PP2A/C and Bcl-x_L dephosphorylation, we

treated ARPE-19 cells with H_2O_2/TNFα in the absence and presence of NPD1. H_2O_2/TNFα treatment altered the interaction of PP2A/Cα with S62Bcl-x_L (Fig. 5*B*), as demonstrated by coimmunoprecipitation with an antibody specifically directed against phospho-S62Bcl-x_L and probed for PP2A/Cα, whereas NPD1 treatment markedly enhanced S62Bcl-x_L/PP2A/Cα interaction (Fig. 5*B*). Lesser amounts of loading (1/5 and 1/1.25) were also used to exclude the possibility that overloading may mask minor changes in PP2A/Cα interaction (Fig. 5*C*). On the other hand, when coimmunoprecipitation was performed using anti-Bcl-x_L antibody, there was basal level interaction of Bcl-x_L/PP2A/Cα in unstimulated cells. This interaction was increased in H_2O_2/TNFα-treated cells, and a further increase was observed in NPD1-treated cells when compared with control (Fig. 5*D*). These observations suggest that NPD1 can promote assembly of phospho Bcl-x_L and PP2A/Cα, which, in turn, may result in the dephosphorylation of Bcl-x_L at Ser-62.

DISCUSSION

Bcl-x_L is a pro-survival member of the Bcl-2 family of proteins that inhibits cell death induced by a number of apoptotic stimuli (40). The Bcl-2 family members each share homology within the BH1–BH4 regions. Bcl-2 and Bcl-x_L contains all four homology regions, Bax lacks the BH4 domain, and Bad lacks all three domains except the BH3 death domain (41). Bcl-x_L is a close homolog of Bcl-2 and is proposed to exert its anti-apoptotic activity in a similar manner. In healthy cells, Bcl-x_L is localized primarily to the mitochondria with a smaller fraction residing in the cytosol (36, 42), and in some cells such as murine thymocytes, it is also localized in the nucleus (18). One of the pro-survival functions of Bcl-x_L is the inhibition of pro-apoptotic Bax (16). Bax is found in both the cytosol and the mitochondria in many culture cells (36, 38). Upon induction of apoptosis, Bcl-x_L and Bax are predominantly membrane-associated (36). Moreover, phosphorylated forms of the Bcl-2 family proteins Bad and Bax are localized exclusively in the cytosol (29, 30). In a spinal cord injury model (43), Bcl-x_L was shown to be present in the endoplasmic reticulum, nuclei, and cytosol, whereas phosphorylated S62Bcl-x_L was absent from the cytosolic fraction in uninjured spinal cord. As early as 15 min after contusion, an up-regulation of the phospho-Bcl-x_L in the cytosol was observed. In PC-12 cells treated with vinblastine, there was a correlation between the cytoplasmic S62Bcl-x_L levels and apoptosis, suggesting that Bcl-x_L phosphorylation is pro-apoptotic (17, 43). In support of this, subcellular fractionation studies in ARPE-19 cells revealed that S62Bcl-x_L was not localized in mitochondrial fractions or in the unstimulated cytosolic fractions. After induction of oxidative stress, S62Bcl-x_L was detected as early as 15 min in the cytosol and gradually increased thereafter up to 60 min (Fig. 4). The overall protein level of Bcl-x_L remained unchanged in the mitochondria, consistent with previous studies (36). In unstimulated cells, Bax was localized in the cytosol, and a smaller fraction was localized in the mitochondria, and upon induction of oxidative stress, a smaller fraction was translocated to the mitochondria at 30 min (Fig. 4).

Apoptosis-promoting agents, including H_2O_2/TNFα, calcium ionophore, A-23187, and IL-1β, can induce the synthesis of NPD1 via the action of a 15-lipoxygenase-1 enzyme (15-LOX-1) (3, 44). However, our understanding of the signaling mechanism(s) by which NPD1 promotes cell survival remains fragmentary. Because NPD1 counteracts oxidative stress-induced apoptosis and also up-regulates the anti-apoptotic protein Bcl-x_L in ARPE-19 cells (3), it was proposed that NPD1 may act at the transcriptional, translational, and post-translational level to regulate the anti-apoptotic activity of Bcl-x_L. In a previous report, it had been shown that after 1 h of serum starvation and 6 h of 400 and 800 μM H_2O_2/TNFα induction, total Bcl-x_L protein was down-regulated, and 50 nM NPD1 up-regulated this protein (4, 5). The activated (phosphorylated) form of this protein has until now not been studied. We report here that 200 μM H_2O_2/TNFα induced the phosphorylation of Bcl-x_L in ARPE-19 cells after 18 h of serum starvation and that NPD1 down-regulated the same (Fig. 1, *A* and *B*). We further demonstrate that NPD1 was not able to down-regulate the phosphorylation of Bcl-x_L at higher concentrations, such as 400 and 600 μM H_2O_2 (Fig. 1*B*). It has also been demonstrated that reactive oxygen species can influence the phosphorylation of Bcl-2 family proteins. An appropriate amount of reactive oxygen species, usually a small amount, activates phosphokinases and increases the intracellular calcium levels (45, 46). However, a large amount induces peroxidation of DNA, proteins, and lipids, resulting in cell impairments (47, 48). Hence, higher concentrations of H_2O_2/TNFα may increase reactive oxygen species levels in ARPE-19 cells, which might decrease the potency of NPD1. Therefore, the effect observed in Fig. 1*B* might be a concentration- and time-dependent phenomenon. Taken together, our data suggest that Bcl-x_L phosphorylation is an early event (>5 min) with a significant up-regulation from 30 to 90 min under the present experimental conditions. After 60 min, the phosphorylation status was reversed to that observed at 30 min (Fig. 1*A*). These observations are consistent with phosphorylation and dephosphorylation events occurring much earlier than the appearance of apoptotic features. We cannot rule out the possibility that a much higher concentration of NPD1 might be effective with an increased concentration of H_2O_2, resulting in a more rapid activation of Bcl-x_L.

Other studies also demonstrate Bcl-x_L phosphorylation at Ser-62 through activation of JNK, thereby inactivating its anti-apoptotic activity (17, 21, 22). Our results demonstrated JNK-mediated activation of S62Bcl-x_L in our model system (data not shown) as well. It is possible that dephosphorylation of Bcl-x_L mediated by a protein phosphatase may also play a role in regulating its anti-apoptotic activity. Our results further suggest that PP2A is able to function as a Bcl-x_L phosphatase because specific disruption of PP2A activity by treatment of ARPE-19 cells with okadaic acid enhanced Bcl-x_L phosphorylation (Fig. 2*A*). Furthermore PP2A expression was observed in the cytosol, consistent with the absence of S62Bcl-x_L. In oxidative stress-induced cells, a down-regulation in the expression pattern of PP2A/C was observed as a function of time, correlating with increased phosphorylation of Bcl-x_L (Fig. 4). PP2A/C also was found to be localized in the mitochondria of control cells, and oxidative stress enhanced the translocation. Importantly, two homologous proteins that noncompetitively inhibit the phosphatase activity of PP2A, I1PP2A and I2PP2A (49, 50), were not

found to be altered in abundance between control or stressed ARPE-19 cells when compared with actin levels in the same sample. These observations are consistent with previous studies demonstrating that C_2-ceramide, an activator of PP2A, mediates dephosphorylation of the Bcl-x_L homolog Bcl-2 by translocating PP2A to the mitochondria (23, 24). Confirmation of PP2A as a Bcl-x_L phosphatase was obtained from the results of transfection studies that demonstrated specific knockdown of PP2A/Cα expression by siRNA-increased Bcl-x_L phosphorylation (Fig. 2*C*), which promoted apoptotic cell death (Fig. 3*C*). In contrast, NPD1 attenuated PP2A/C-mediated cell death (Fig. 3*C*). Moreover, NPD1 enhanced the interaction between S62Bcl-x_L and PP2A/Cα in H_2O_2/TNFα-induced ARPE-19 cells (Fig. 5*B*), supporting the notion that NPD1-stimulated Bcl-x_L/Bax interaction (Fig. 5*A*) is associated with the increased availability of total Bcl-x_L, presumably on the mitochondrial membrane. It is possible that these interactions disable the pro-apoptotic protein Bax from forming oligomers, thus inhibiting the formation of ion channels on the mitochondria and thus releasing cytochrome *c* into the cytosol.

It has been also demonstrated that PP2A, specifically PP2A/C, can dephosphorylate the Bcl-x_L homolog Bcl-2 by directly binding to its BH4 domain (29). Pro-survival Bcl-2 family members possess a conserved BH4 domain, and deletion of this domain presumably converts Bcl-2 to a multidomain Bax-like death effector (51, 52), suggesting that the BH4 domain is critical for anti-apoptotic activity. Taken together, we propose that the BH4 domain of Bcl-x_L might function as the PP2A "docking site" and a potential bridge for PP2A to access the Ser-62 phosphorylation site located in the loop region adjacent to the N-terminal BH4 domain. This mechanism may contribute to removal of the phosphate of Bcl-x_L, leading to inhibition of its pro-apoptotic function.

In related studies, the sphingolipid ceramide, which exerts its effect at the subcellular site of production, has been shown to stimulate PP2A activity by binding to the catalytic domain of PP2A (24, 49, 53, 54). We demonstrate that the omega-3 fatty acid derivative, NPD1, increases PP2A activity (Fig. 3*A*) and also that NPD1 synthesis is a near universal response to oxidative stress because of its ability to inactivate apoptotic signaling at the mitochondrial level (3, 4). The present study shows that NPD1 can induce dephosphorylation of Bcl-x_L in a PP2A-dependent manner and promote ARPE-19 cell survival. Our results also indicate that NPD1 facilitation of PP2A interaction with S62Bcl-x_L (Fig. 5*B*) might increase the dephosphorylation of Bcl-x_L and promote Bax/Bcl-x_L heterodimerization (Fig. 5*A*). That NPD1 may facilitate a direct Bax/Bcl-x_L interaction through additional regulatory mechanisms can, at this time, not be excluded.

Our findings and the demonstration of the involvement of the BH4 domain (a feature inherent only with the anti-apoptotic proteins) in PP2A docking (29) indicate a novel mechanism for NPD1-induced cell survival. NPD1-stimulated Bcl-x_L dephosphorylation and/or PP2A-induced dephosphorylation might mediate a conformational change in Bcl-x_L resulting in exposure of its BH3 domain, which is normally hidden in the hydrophobic domain of Bcl-x_L (55). Thus, NPD1-induced Bcl-x_L dephosphorylation may activate Bcl-x_L via a conformational change in the BH3 domain that promotes Bax and Bcl-x_L association, and NPD1-activated PP2A may more efficiently facilitate heterodimerization of Bax and Bcl-x_L.

Taken together, these findings are significant for several reasons. First, the observation of NPD1-induced dephosphorylation of S62Bcl-x_L defines a mechanism of controlling the expression of anti- and pro-apoptotic factors in response to oxidative stress. Second, a specific and direct mechanism mediated by an NPD1-activated protein phosphatase has been established in RPE cells. Moreover, NPD1 attenuates laser-induced choroidal neovascularization *in vivo* in an experimental model of age-related macular degeneration (56).

In summary, we demonstrate that Bcl-x_L phosphorylation in ARPE-19 cells is induced by oxidative stress and that NPD1 enhances PP2A activity, in turn attenuating oxidative stress-induced phosphorylation of the anti-apoptotic protein Bcl-x_L. These studies, for the first time, identify NPD1 as a novel regulator of the PP2A/C/Bcl-x_L interaction. Hence, our results establish a stimulus-specific response in NPD1-dependent phosphorylation of Bcl-x_L. NPD1 modulates the activation of this Bcl-2 family member by changing the phosphorylation status in a PP2A-dependent manner and also by enhancing the interaction of its counterpart, pro-apoptotic protein Bax, suggesting a highly coordinated, NPD1-mediated regulation of cell survival in response to oxidative stress.

REFERENCES

1. Bok, D. (2007) *Arch. Ophthalmol.* **125,** 160–164
2. Strauss, O. (2005) *Physiol. Rev.* **85,** 845–881
3. Mukherjee, P. K., Marcheselli, V. L., Serhan, C. N., and Bazan, N. G. (2004) *Proc. Natl. Acad. Sci. U.S.A.* **101,** 8491–8496
4. Mukherjee, P. K., Marcheselli, V. L., Barreiro, S., Hu, J., Bok, D., and Bazan, N. G. (2007) *Proc. Natl. Acad. Sci. U.S.A.* **104,** 13152–13157
5. Mukherjee, P. K., Marcheselli, V. L., de Rivero Vaccari, J. C., Gordon, W. C., Jackson, F. E., and Bazan, N. G. (2007) *Proc. Natl. Acad Sci. U.S.A.* **104,** 13158–13163
6. Marcheselli, V. L., Mukherjee, P. K., Arita, M., Hong, S., Antony, R., Sheets, K., Winkler, J. W., Petasis, N. A., Serhan, C. N., and Bazan, N. G. (2010) *Prostaglandins Leukot. Essent. Fatty Acids* **82,** 27–34
7. Serhan, C. N., Yacoubian, S., and Yang, R. (2008) *Annu. Rev. Pathol.* **3,** 279–312
8. Marcheselli, V. L., Hong, S., Lukiw, W. J., Tian, X. H., Gronert, K., Musto, A., Hardy, M., Gimenez, J. M., Chiang, N., Serhan, C. N., and Bazan, N. G. (2003) *J. Biol. Chem.* **278,** 43807–43817
9. Bazan, N. G. (2007) *Invest. Ophthalmol. Vis. Sci.* **48,** 4866–4881
10. Lukiw, W. J., Cui, J. G., Marcheselli, V. L., Bodker, M., Botkjaer, A., Gotlinger, K., Serhan, C. N., and Bazan, N. G. (2005) *J. Clin. Invest.* **115,** 2774–2783
11. Hollyfield, J. G. (2010) *Invest. Ophthalmol. Vis. Sci.* **51,** 1275–1281
12. Hollyfield, J. G., Bonilha, V. L., Rayborn, M. E., Yang, X., Shadrach, K. G., Lu, L., Ufret, R. L., Salomon, R. G., and Perez, V. L. (2008) *Nat. Med.* **14,** 194–198
13. Bazan, N. G. (2006) *Trends Neurosci.* **29,** 263–271
14. Lotery, A., and Trump, D. (2007) *Hum. Genet.* **122,** 219–236
15. Kim, R. (2005) *Biochem. Biophys. Res. Commun.* **333,** 336–343
16. Yang, E., Zha, J., Jockel, J., Boise, L. H., Thompson, C. B., and Korsmeyer, S. J. (1995) *Cell* **80,** 285–291
17. Basu, A., and Haldar, S. (2003) *FEBS Lett.* **538,** 41–47
18. Sedlak, T. W., Oltvai, Z. N., Yang, E., Wang, K., Boise, L. H., Thompson, C. B., and Korsmeyer, S. J. (1995) *Proc. Natl. Acad. Sci. U.S.A.* **92,** 7834–7838
19. Minn, A. J., Kettlun, C. S., Liang, H., Kelekar, A., Vander Heiden, M. G., Chang, B. S., Fesik, S. W., Fill, M., and Thompson, C. B. (1999) *EMBO J.* **18,**

632–643
20. Schmitt, E., Beauchemin, M., and Bertrand, R. (2007) *Oncogene* **26,** 5851–5865
21. Basu, A., and Haldar, S. (2008) *Int. J. Oncol.* **33,** 657–663
22. Upreti, M., Galitovskaya, E. N., Chu, R., Tackett, A. J., Terrano, D. T., Granell, S., and Chambers, T. C. (2008) *J. Biol. Chem.* **283,** 35517–35525
23. Tamura, Y., Simizu, S., and Osada, H. (2004) *FEBS Lett.* **569,** 249–255
24. Ruvolo, P. P., Deng, X., Ito, T., Carr, B. K., and May, W. S. (1999) *J. Biol. Chem.* **274,** 20296–20300
25. Chiang, C. W., Harris, G., Ellig, C., Masters, S. C., Subramanian, R., Shenolikar, S., Wadzinski, B. E., and Yang, E. (2001) *Blood* **97,** 1289–1297
26. Parsons, R. (1998) *Curr. Opin. Oncol.* **10,** 88–91
27. McCright, B., Rivers, A. M., Audlin, S., and Virshup, D. M. (1996) *J. Biol. Chem.* **271,** 22081–22089
28. Sontag, E., Nunbhakdi-Craig, V., Bloom, G. S., and Mumby, M. C. (1995) *J. Cell Biol.* **128,** 1131–1144
29. Deng, X., Gao, F., and May, W. S. (2009) *Blood* **113,** 422–428
30. Xin, M., and Deng, X. (2006) *J. Biol. Chem.* **281,** 18859–18867
31. Boon-Unge, K., Yu, Q., Zou, T., Zhou, A., Govitrapong, P., and Zhou, J. (2007) *Chem. Biol.* **14,** 1386–1392
32. Benito, A., Lerga, A., Silva, M., Leon, J., and Fernandez-Luna, J. L. (1997) *Leukemia* **11,** 940–944
33. Cook, S. A., Sugden, P. H., and Clerk, A. (1999) *Circ. Res.* **85,** 940–949
34. Valks, D. M., Kemp, T. J., and Clerk, A. (2003) *J. Biol. Chem.* **278,** 25542–25547
35. Kim, M. J., Futai, K., Jo, J., Hayashi, Y., Cho, K., and Sheng, M. (2007) *Neuron* **56,** 488–502; Correction (2008) *Neuron* **57,** 320–327
36. Hsu, Y. T., Wolter, K. G., and Youle, R. J. (1997) *Proc. Natl. Acad. Sci. U.S.A.* **94,** 3668–3672
37. Er, E., Lalier, L., Cartron, P. F., Oliver, L., and Vallette, F. M. (2007) *J. Biol. Chem.* **282,** 24938–24947
38. Hsu, Y. T., and Youle, R. J. (1997) *J. Biol. Chem.* **272,** 13829–13834
39. Simizu, S., Tamura, Y., and Osada, H. (2004) *Cancer Sci.* **95,** 266–270
40. Grillot, D. A., González-García, M., Ekhterae, D., Duan, L., Inohara, N., Ohta, S., Seldin, M. F., and Nuñez, G. (1997) *J. Immunol.* **158,** 4750–4757
41. Zhou, H., Hou, Q., Chai, Y., and Hsu, Y. T. (2005) *Exp. Cell Res.* **309,** 316–328
42. Thuduppathy, G. R., Craig, J. W., Kholodenko, V., Schon, A., and Hill, R. B. (2006) *J. Mol. Biol.* **359,** 1045–1058
43. Cittelly, D. M., Nesic-Taylor, O., and Perez-Polo, J. R. (2007) *J. Neurosci. Res.* **85,** 1894–1911
44. Calandria, J. M., Marcheselli, V. L., Mukherjee, P. K., Uddin, J., Winkler, J. W., Petasis, N. A., and Bazan, N. G. (2009) *J. Biol. Chem.* **284,** 17877–17882
45. Rothstein, E. C., Byron, K. L., Reed, R. E., Fliegel, L., and Lucchesi, P. A. (2002) *Am. J. Physiol. Heart Circ. Physiol.* **283,** H598–H605
46. Benhar, M., Dalyot, I., Engelberg, D., and Levitzki, A. (2001) *Mol. Cell Biol.* **21,** 6913–6926
47. Covacci, V., Torsello, A., Palozza, P., Sgambato, A., Romano, G., Boninsegna, A., Cittadini, A., and Wolf, F. I. (2001) *Chem. Res. Toxicol.* **14,** 1492–1497
48. Dröge, W. (2002) *Physiol. Rev.* **82,** 47–95
49. Li, M., Makkinje, A., and Damuni, Z. (1996) *Biochemistry* **35,** 6998–7002
50. Kovacech, B., Kontsekova, E., Zilka, N., Novak, P., Skrabana, R., Filipcik, P., Iqbal, K., and Novak, M. (2007) *FEBS Lett.* **581,** 617–622
51. Cheng, E. H., Kirsch, D. G., Clem, R. J., Ravi, R., Kastan, M. B., Bedi, A., Ueno, K., and Hardwick, J. M. (1997) *Science* **278,** 1966–1968
52. Reed, J. C., Zha, H., Aime-Sempe, C., Takayama, S., and Wang, H. G. (1996) *Adv. Exp. Med. Biol.* **406,** 99–112
53. Law, B., and Rossie, S. (1995) *J. Biol. Chem.* **270,** 12808–12813
54. Kolesnick, R. N., and Krönke, M. (1998) *Annu. Rev. Physiol.* **60,** 643–665
55. Muchmore, S. W., Sattler, M., Liang, H., Meadows, R. P., Harlan, J. E., Yoon, H. S., Nettesheim, D., Chang, B. S., Thompson, C. B., Wong, S. L., Ng, S. L., and Fesik, S. W. (1996) *Nature* **381,** 335–341
56. Sheets, K. G., Zhou, Y., Ertel, M. K., Knott, E. J., Regan, C. E., Jr., Elison, J. R., Gordon, W. C., Gjorstrup, P., and Bazan, N. G. (2010) *Mol. Vis.* **2,** 320–329